Nanostructures

Germanium-Catalyzed Growth of Zinc Oxide Nanowires: A Semiconductor Catalyst for Nanowire Synthesis**

*Zheng Wei Pan, Sheng Dai, Christopher M. Rouleau, and Douglas H. Lowndes**

The vapor–liquid–solid (VLS) crystal growth mechanism, first proposed by Wagner and Ellis in 1964 for Si-whisker growth,[1] has been widely used to guide the growth of a wide range of nanowires, such as Group IV (such as Si and Ge),[2–7] III–V (such as GaAs and InP),[5,6] and II–VI (such as ZnS and ZnSe)[5,7] semiconductors, and oxides (such as ZnO and SiO_2).[8–10] In this mechanism, a catalyst nanoparticle serves as a preferential site for the absorption and dissolution of reactants from the vapor phase, directs the nanowire's growth direction, and defines the diameter of the nanowire. A common morphological feature of VLS-grown nanowires is that each nanowire is terminated at one end by a catalyst nanoparticle with a diameter similar to that of the nanowire. The catalysts used so far are usually metals, with the most popular ones being gold[3–9] and iron.[2]

ZnO is recognized as a promising photonic material in the blue-ultraviolet (UV) region due to its wide bandgap (3.37 eV) and large exciton binding energy (60 meV). Stimulated by recent reports of room-temperature UV lasing from ZnO nanowires,[9] ZnO, in the form of nanowires, nanorods, and nanobelts, is attracting a great deal of attention from the research community. Various methods have been developed for synthesizing these one-dimensional ZnO nanostructures, such as metal-catalyzed VLS growth,[8,9,11] physical vapor deposition,[12–14] chemical vapor deposition (CVD),[15] metal-organic vapor-phase epitaxy,[16] metalorganic CVD,[17] template-assisted growth,[18] and various solution methods.[19,20] Among these techniques, metal-catalyzed VLS growth has the advantage of allowing the controlled and patterned growth of ZnO nanowires,[8,9,11] and yields nanowires from well-defined and/or patterned sites on surfaces that could facilitate the integration of ZnO nanowires for characterization and their use in devices.

We report here that Ge, a Group IV semiconductor, can be used as an efficient catalyst for high-yield growth of very long (up to several hundred micrometers), extremely straight, and quasi-aligned arrays of single-crystalline ZnO nanowires in a VLS process. The Zn source was generated by carbothermal reduction of ZnO powder. The Ge catalyst was provided either by the vapor, generated by carbothermal reduction of GeO_2 powder, or by patterning Ge dots on a SiO_2-coated Si wafer by photolithography. Several kinds of substrates were used for nanowire growth, such as alumina plates, sapphire wafers, silicon wafers, and copper grids.

Figure 1 a shows a low-magnification scanning electron microscopy (SEM) image of the ZnO nanowires grown on an alumina substrate. A white layer of high-density ZnO nanowires with a uniform thickness of about 150 μm has formed on the substrate surface. The nanowires tend to grow normal to the substrate surface to form a quasi-aligned nanowire array (Figure 1 b). They are well-faceted with hexagonal cross-sections (Figure 1 c, d), which indicates that the Wurtzite-type

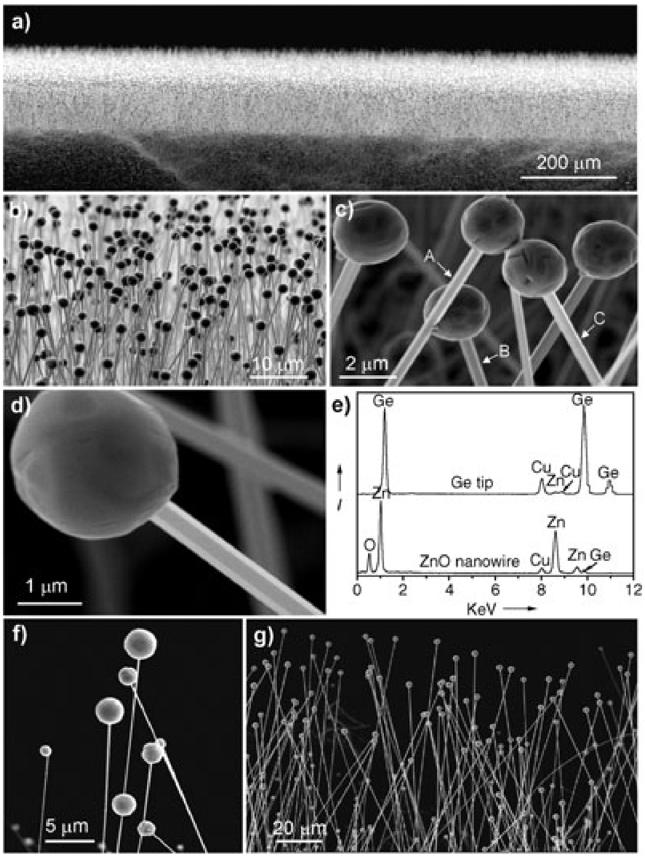

Figure 1. SEM and EDS characterization of Ge-catalyzed ZnO nanowires. a–d) SEM images of a long, straight ZnO nanowire array grown on an alumina substrate. The nanowires are terminated at their upper ends with large Ge particles. e) EDS spectra recorded at the tip and trunk of the Ge-particle-terminated ZnO nanowires. The spectra were recorded with a TEM. The Cu peaks are from the copper TEM grid. f) An SEM image showing similar-sized nanowires catalyzed by different-sized Ge particles. g) Straight ZnO nanowire arrays grown on a sapphire substrate.

---

[*] Dr. Z. W. Pan, Dr. C. M. Rouleau, Dr. D. H. Lowndes
Condensed Matter Sciences Division
Oak Ridge National Laboratory
Oak Ridge, TN 37831-6056 (USA)
Fax: (+1) 865-576-5235
E-mail: lowndesdh@ornl.gov

Dr. S. Dai
Chemical Sciences Division
Oak Ridge National Laboratory
Oak Ridge, TN 37831-6201 (USA)

[**] This research was sponsored by the Office of Basic Energy Science of the US Department of Energy (DOE) and the Laboratory Directed Research and Development Program of Oak Ridge National Laboratory (ORNL). The research was carried out at the ORNL, managed by UT-Battelle, LLC, for the US DOE under contract no. DE-AC05-00OR22725. We thank the ORNL SHaRE Collaborative Research Center for the use of their electron facilities. We are also grateful to Dr. D. B. Beach and Dr. N. D. Evans for helpful discussions.

DOI: 10.1002/ange.200460043

ZnO nanowires grow along the ⟨0001⟩ direction. One unique feature of our nanowires is that they are terminated at their growing ends by very large spherical particles with diameters of up to several micrometers. The presence of particles at the ends of the nanowires is suggestive of a VLS growth process.[1–3] Indeed, as shown in Figure 1c, the fact that wire A slices the tip of wire B, and that the tips of wire A and wire C are stuck together, strongly suggests that the large particles were in the liquid or semi-solid state during the growth. Energy-dispersive X-ray spectroscopy (EDS) analyses conducted with a transmission electron microscope (TEM) show that the particles are Ge with traces of Zn, whereas the nanowires contain Zn and O with traces of Ge (<1 atom %) (Figure 1e). This indicates that the particles atop the nanowires are Ge and that the nanowires are Ge-doped ZnO. We therefore conclude that our ZnO nanowires grow by a Ge-catalyzed VLS process. To the best of our knowledge, this is the first example of a nonmetal catalyzing nanowire growth. (Note that Ge has been used before as a growth medium in the synthesis of millimeter-scale GaAs whiskers, but it was subsequently found to be present in the core and throughout the entire length of the whisker.[21])

The Ge-catalyzed ZnO nanowires are very straight and very little curvature was observed over the full length of some of the hundreds-of-micrometers-long nanowires. Detailed SEM investigations across the entire nanowire growth region showed that, within the nanowire formation regime (500–650 °C), the sizes of both the nanowires and the Ge particles increase with temperature. After 30 min of growth, the diameters and lengths of the nanowires are in the ranges 50–400 nm and 50–200 μm, respectively. The diameters of the Ge particles, however, vary from 0.5 to 4 μm, about 5–15 times those of the associated nanowires. These Ge-particle diameters are much larger than for metal-catalyzed nanowire growth, for which the diameters of the catalyst particles are similar to those of the nanowires.[2–6] The present nanowires grow very rapidly, with rates of up to 400 $\mu m\,h^{-1}$ at a growth temperature of about 600 °C; this is about one order of magnitude faster than Au-catalyzed ZnO nanowire growth.[8,9] Unlike metal-catalyzed nanowire growth, in which the diameter of the nanowires is mainly determined by the size of the catalyst particles,[2–6] it seems that the diameter of the Ge-catalyzed ZnO nanowires is less influenced by the Ge particle size. For example, as shown in Figure 1f, the nanowires that result from a 3.5-μm-diameter Ge particle (the largest one) and a 1-μm-diameter Ge particle (the smallest one) have essentially the same diameter (~100 nm). This may explain the fact that even though the Ge particle grows up with time by continuously absorbing Ge species from the vapor, the diameter of each nanowire is almost constant over most of its length. (Note that a tapered morphology can be observed over the first few micrometers of the nanowires, probably due to the significant increase of the size of the Ge particle at the initial growth stage.)

The Ge-catalyzed ZnO nanowire growth is substrate independent. Besides alumina substrates, ZnO nanowires were also grown on sapphire and silicon wafers, and even on copper TEM grids. Figure 1g is an SEM image of ZnO nanowires grown on a sapphire wafer. It shows long (up to 100 μm), very straight, and quasi-aligned ZnO nanowires that terminate in large Ge particles. Figure 2a is a low-magnification SEM image of ZnO nanowires grown on the bars of a copper TEM grid consisting of hexagonal windows. In each hexagonal window straight ZnO nanowires tend to grow along the surface normal of each edge of the hexagon; they converge upon the window center (Figure 2b). Such a growth phenomenon was also observed on a TEM grid consisting of square windows (Figure 2c).

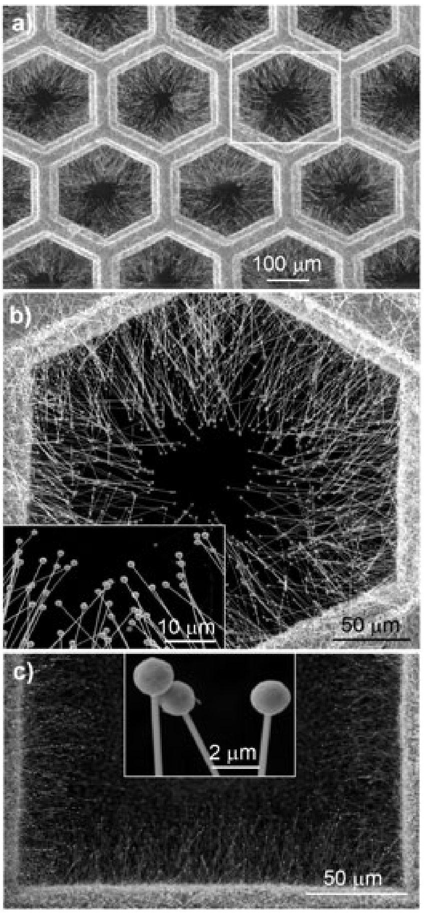

Figure 2. SEM images of Ge-catalyzed ZnO nanowires grown on copper TEM grids. a) Low-magnification SEM image of ZnO nanowires grown on a copper grid with hexagonal windows. b) An enlargement of the boxed region in Figure 2a. The inset shows a high-magnification image of the nanowires. c) An SEM image of ZnO nanowires grown on a copper grid with square windows. The inset shows a high-magnification image of the nanowires.

TEM studies of the ZnO nanowires provide further insight into the morphology of these materials. Figure 3a and b show the TEM images of the ZnO nanowires grown directly on TEM grids. It is clear that the nanowires are very straight, have a uniform diameter along their axes, and terminate in large spherical Ge particles. High-resolution TEM investigations show that the ZnO nanowires are structurally uniform and single crystalline. Figure 3c is a high-resolution TEM image of a thin, single-crystalline ZnO nanowire, and Figure 3d is an atomic-resolution image of the surface of a nanowire. These images clearly show the (0001) atomic planes

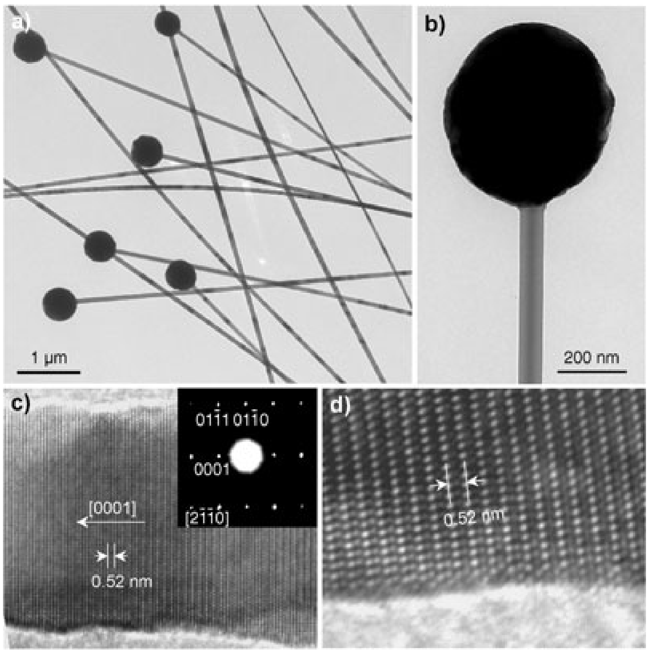

Figure 3. TEM and high-resolution TEM images of Ge-catalyzed ZnO nanowires. a,b) TEM images of ZnO nanowires grown directly on the TEM grid, showing straight and uniform nanowires terminating in large Ge particles. c) High-resolution TEM image of a thin ZnO nanowire. The inset is an electron-diffraction pattern of the crystalline nanowire recorded along the $[2\bar{1}\bar{1}0]$ zone axis. d) An atomic-resolution image showing a clean and structurally perfect nanowire surface.

(separation: 0.52 nm) perpendicular to the nanowire axis, thus indicating that $\langle 0001\rangle$ is the preferred growth direction of these Wurtzite-type ZnO nanowires. The single-crystal nature of the nanowires and their $\langle 0001\rangle$ growth direction were confirmed by the electron-diffraction pattern recorded perpendicular to the nanowire's long axis, as shown in the inset of Figure 3c, which could be indexed as the $[2\bar{1}\bar{1}0]$ zone axis of crystalline ZnO. The surfaces of the nanowires are clean, atomically sharp, and without any amorphous sheathed phase (Figure 3d).

In metal-catalyzed semiconductor nanowire growth, binary or pseudobinary phase diagrams are usually used to predict catalysts and growth conditions.[2,5] Although no Ge–ZnO phase diagram is available, this principle can be rationally applied to the present Ge-catalyzed ZnO nanowire growth by considering both the conventional Ge–Zn binary phase diagram[22] and the in-situ oxidation of Zn into ZnO during growth.[8] The Ge–Zn phase diagram is characterized by a eutectic reaction at 394 °C and 94.2 atom% Zn. This implies that a Ge-catalyzed VLS-type process can take place if the concentration of Zn is higher than 94.2 atom%. Such high-Zn-content Ge–Zn droplets can be readily formed since in the source materials the amount of ZnO present is about 10 times that of GeO$_2$ (molar ratio). When the droplets become supersaturated, ZnO nanowires are formed, possibly by the in situ reaction between Zn and a small amount of CO/O$_2$ present in the reaction chamber, as happens in Au-catalyzed ZnO nanowire growth.[8] The CO gas is formed by the carbothermal reduction of ZnO and GeO$_2$, whereas the oxygen mainly originates from leaks in our reaction system.[10]

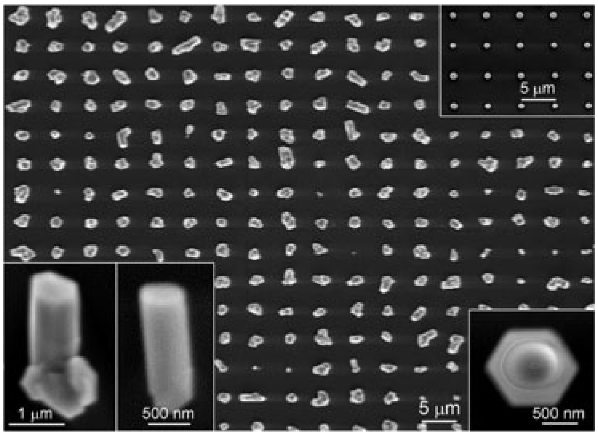

Figure 4. SEM images of a ZnO nanorod pattern grown on a Ge-dot pattern. The top-right inset shows the Ge-dot pattern. The bottom-left insets show two typical morphologies of the nanorods. The bottom-right inset is the top view of a hexagonal nanorod, showing a hemispherical hollow at the upper end of the nanorod.

For the Ge-catalyzed ZnO nanowire growth reported above, Ge was fed from the vapor, and the Ge catalyst particles formed on the substrate surface at the initial growth stage were randomly distributed. However, recent studies on metal-catalyzed VLS nanowire growth have shown that the controlled growth of nanowires at certain locations can be achieved from well-defined metal-catalyst particles on substrate surfaces.[4,8,9] To achieve such controlled growth from Ge, and to verify the catalytic effect of Ge on ZnO growth, we patterned uniformly sized Ge dots (~0.5 µm in diameter and 75 nm thick), with a spacing of about 5 µm, on a SiO$_2$-coated Si wafer by photolithography (Figure 4, upper inset), and carried out ZnO growth. Subsequent SEM studies (Figure 4) revealed the formation of a ZnO nanorod array that conforms to the Ge-dot pattern with high fidelity; the region without Ge dots remains completely clean. These observations clearly demonstrate the feasibility of highly deterministic control of ZnO nanowire growth at predetermined Ge-dot locations, as well as the catalytic capability of Ge for ZnO nanorod array synthesis. However, the nanorods in Figure 4 are much shorter (< 2 µm) than the nanowires described above, and no Ge particles were observed at the nanorod tips after the growth experiment at 900 °C for 1 h. This may be explained by considering the different sources of Ge and evolution of Ge particle sizes in these two kinds of syntheses. For the growth shown in Figure 1–3, the Ge particles can grow (up to 4 µm) by continuously absorbing Ge species from the vapor, so that they have sufficient volume to absorb Zn and O species to sustain fast growth of long ZnO nanowires. In contrast, for the Ge-dot pattern the Ge dots' initial volume is only about 3% of that of even a 1-µm-diameter Ge particle, and therefore the Ge dots decrease in size, and finally disappear, due to the continuous evaporation of Ge without replenishment. This process results in a much lower growth rate and short ZnO nanorods. Indeed, hemispherical hollows with diameters similar to those of the original Ge dots were usually observed at the top ends of the nanorods (Figure 4, bottom right inset). These are possibly left by the evaporated Ge dots, thus confirming this model. Further work is underway to deterministically grow ZnO nanowires with controllable lengths and locations using a variety of well-defined Ge dots.

The photoluminescence (PL) spectra of the Ge-catalyzed ZnO nanowires were measured by using a Xe lamp (325 nm) as the excitation source. Figure 5 shows a room-temperature PL spectrum recorded from the ZnO nanowires grown on an alumina substrate. An intense UV emission at 378 nm and a weak, broader green emission peaking at about 490 nm were detected. While the UV-band emission corresponds to the near-band-edge free excitonic emission, the green-band emission is commonly referred to as deep-level or trap-state emission.[8] The observation of an intense free-exciton peak at room temperature strongly suggests that the Ge-catalyzed ZnO nanowires are of high optical quality. The origin of the deep-level emission in ZnO is not yet clearly understood, but is generally attributed to singly ionized oxygen vacancies[23] and extrinsic impurities.[24,25] Since our ZnO nanowires are structurally uniform and single crystalline, the weak green emission presumably arises mainly from the trace amount of Ge present in the nanowires, which could provide the green luminescence by either donor–acceptor pair or donor–hole recombination.[24,25]

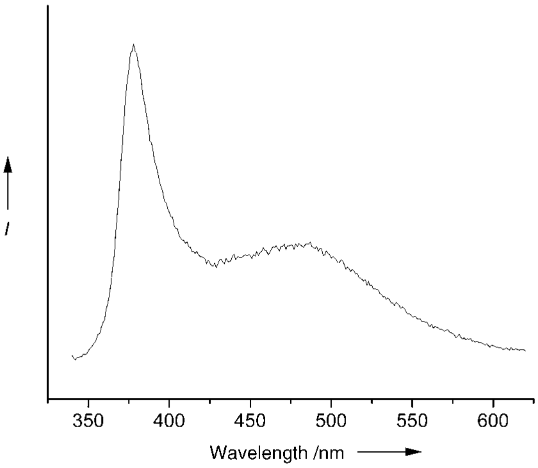

Figure 5. Photoluminescence spectrum of ZnO nanowires showing an intense UV emission at 378 nm and a weak green emission peaking at about 490 nm.

Taken together, the above results show that semiconductor Ge can act as an efficient catalyst for high-yield growth of very long, extremely straight, and quasi-aligned arrays of single-crystalline ZnO nanowires by a VLS process. The use of Ge as the catalyst enriches and broadens the current understanding of the conventional VLS nanowire growth mechanism in which metals have generally been used as the catalysts. Our results suggest that it should be possible to prepare nanowires of other oxides or of compound semiconductors by using Ge or other nonmetallic elements as the catalysts. Moreover, the ZnO nanowires and synthesis methods reported here could offer opportunities for further fundamental research as well as technological applications. For example, it should be readily possible to apply electrodes to these straight and long nanowires for transport measurements, and the deterministic growth may have important practical implications, for example, for near-UV light emitting arrays.

Experimental Section

Nanowire synthesis: The ZnO nanowires were synthesized in a tube furnace system[10] by carbothermal reduction of ZnO powder in the presence of semiconductor Ge as the catalyst. The Ge catalyst was provided either from the vapor generated by carbothermal reduction of GeO_2 powder or by patterning Ge dots on a SiO_2-coated silicon wafer by photolithography. For the syntheses in which Ge was provided from the vapor, ZnO powder, carbon black, and GeO_2 powder (1:1:0.1 molar ratio) were ground together and transferred into an alumina boat. The boat was then positioned at the center of an alumina tube that was inserted into a horizontal tube-furnace. Several alumina (or silicon wafer or sapphire wafer) strips ($30 \times 10\,mm^2$) were placed downstream one-by-one to act as nanowire-growth substrates. The starting materials were then heated to 900 °C under an argon atmosphere at a flow rate of 50 sccm and a pressure of about 250 Torr for 30 min. The reactant vapors (Zn, Ge, CO, and O species) generated by carbothermal reduction of ZnO and GeO_2 were carried and transported by the argon flow to the substrates, where ZnO nanowires grew. After the furnace had cooled down to room temperature, ZnO nanowires were found on all exposed surfaces (including the top surface and four side surfaces) of the substrates located in the region at temperatures of about 500–650 °C.

For the patterned growth of ZnO nanowires, the Ge-dot patterns were prepared by photolithography using a GCA Autostep 200 *i*-line stepper system.[26] A 4-inch Si wafer coated with a 1-μm-thick SiO_2 layer was used as the substrate. The wafer was spin-coated with approximately 500 nm of photoresist (Shipley Megaposit 955-CM 0.9) at 6000 rpm for 30 s. After baking at 90 °C for 90 s, the wafer was exposed using a step size of 15 mm and a 25 × 25 mm aperture. At 5 × reduction, we obtained a 5 × 5 array of 5 × 5 mm die on a 15 mm pitch. After exposure, the wafer was baked at 120 °C for 90 s, developed for 60 s (Shipley Microposit MF-CD-26), and then reactive-ion-etched for 30 s ($308\,mW\,cm^{-2}$ with 0.1 Torr O_2 at 50 sccm) to eliminate the photoresist residue. At this stage, the wafer had many small windows (~ 0.5 μm in diameter on a 5 μm pitch) within the photoresist and was ready for metallization. A 75-nm-thick layer of Ge was then deposited onto the patterned substrate at room temperature by electron-beam evaporation. Finally, liftoff was performed by soaking the wafer in acetone to remove all the unnecessary Ge, leaving a 5 × 5 array of 5 × 5 mm squares on a 15 mm pitch. Within each square there was an array of Ge dots with a diameter of 0.5 μm, a thickness of 75 nm, and a spacing of 5 μm, as shown in the upper inset of Figure 4.

The Ge-dot-patterned substrates were then loaded onto a 20-cm-long graphite crucible filled with equal amounts of ZnO powder and carbon black, with the catalyst side facing down and a vertical distance between the Zn source and substrates of about 3–5 mm. The growth was conducted at 900 °C for 1 h in an argon flow. During these experiments, we noted that rodlike ZnO nanostructures were grown only on the Ge-dot patterns located in the region at a temperature of about 650–800 °C, about 150 °C higher than the nonpatterned growth described above. Below about 650 °C, no ZnO nanorods were grown, and the Ge-dot patterns seemed unchanged. Above about 800 °C, however, the Ge dots evaporated completely and thus no nanorods were formed.

Characterization: The morphology of the as-synthesized nanowires was examined with a Philips XL-30 SEM operating at 10 kV.

The microstructure was characterized with a Philips CM200 high-resolution TEM operating at 200 kV. The composition of the nanowires was analyzed by an energy-dispersive X-ray spectrometer attached to the TEM. The photoluminescence study was carried out at room temperature on a SPEX Fluorolog-3 spectrofluorometer using a Xe lamp as the excitation source. The excitation wavelength was 325 nm.

Received: March 18, 2004
Revised: September 23, 2004

Keywords: catalyst · germanium · nanostructures · semiconductors

---

[1] R. S. Wagner, W. C. Ellis, *Appl. Phys. Lett.* **1964**, *4*, 89.
[2] A. M. Morales, C. M. Lieber, *Science* **1998**, *279*, 208.
[3] J. Westwater, D. P. Gosain, S. Tomiya, S. Usui, H. Ruda, *J. Vac. Sci. Technol. B* **1997**, *15*, 554.
[4] D. W. Wang, H. J. Dai, *Angew. Chem.* **2002**, *114*, 4977; *Angew. Chem. Int. Ed.* **2002**, *41*, 4783.
[5] X. F. Duan, C. M. Lieber, *Adv. Mater.* **2000**, *12*, 298.
[6] M. S. Gudiksen, J. F. Wang, C. M. Lieber, *J. Phys. Chem. B* **2001**, *105*, 4062.
[7] Y. W. Wang, L. D. Zhang, C. H. Liao, G. Z. Wang, S. S. Peng, *Chem. Phys. Lett.* **2002**, *357*, 314.
[8] M. H. Huang, Y. Y. Wu, H. Feick, N. Tran, E. Weber, P. D. Yang, *Adv. Mater.* **2001**, *13*, 113.
[9] M. H. Huang, S. Mao, H. Feick, H. Q. Yan, Y. Y. Wu, H. Kind, E. Weber, R. Russo, P. D. Yang, *Science* **2001**, *292*, 1897.
[10] Z. W. Pan, Z. R. Dai, C. Ma, Z. L. Wang, *J. Am. Chem. Soc.* **2002**, *124*, 1817.
[11] H. T. Ng, J. Li, M. K. Smith, P. Nguyen, A. Cassell, J. Han, M. Meyyappan, *Science* **2003**, *300*, 1249.
[12] Z. W. Pan, Z. R. Dai, Z. L. Wang, *Science* **2001**, *291*, 1947.
[13] Y. C. Kong, D. P. Yu, B. Zhang, W. Fang, S. Q. Feng, *Appl. Phys. Lett.* **2001**, *78*, 407.
[14] S. C. Lyu, Y. Zhang, H. Ruh, H. J. Lee, H. W. Shim, E. K. Suh, C. J. Lee, *Chem. Phys. Lett.* **2002**, *363*, 134.
[15] J. J. Wu, S. C. Liu, *Adv. Mater.* **2002**, *14*, 215.
[16] W. I. Park, D. H. Kim, S. W. Jung, G. C. Yi, *Appl. Phys. Lett.* **2002**, *80*, 4232.
[17] B. P. Zhang, N. T. Binh, Y. Segawa, K. Wakatsuhi, N. Usami, *Appl. Phys. Lett.* **2003**, *83*, 1635.
[18] Y. Li, G. W. Meng, L. D. Zhang, F. Phillipp, *Appl. Phys. Lett.* **2000**, *76*, 2011.
[19] Z. R. Tian, J. A. Voigt, J. Liu, B. Mckenzie, M. J. Mcdermott, M. A. Rodriguez, H. Konishi, H. F. Xu, *Nat. Mater.* **2003**, *2*, 821.
[20] L. Vayssieres, *Adv. Mater.* **2003**, *15*, 464.
[21] S. Iida, Y. Sugita, *Appl. Phys. Lett.* **1964**, *8*, 77.
[22] T. B. Massalski, *Binary Alloy Phase Diagrams*, *Vol. 2*, 2nd ed., ASM International, New York, **1990**, p. 2023.
[23] K. Vanheusden, W. L. Warren, C. H. Seager, D. R. Tallant, J. A. Voigt, B. E. Gnade, *J. Appl. Phys.* **1996**, *79*, 7983.
[24] R. Dingle, *Phys. Rev. Lett.* **1969**, *23*, 579.
[25] N. Y. Garces, L. Wang, L. Bai, N. G. Giles, L. E. Halliburton, G. Cantwell, *Appl. Phys. Lett.* **2002**, *81*, 622.
[26] M. A. Guillorn, M. L. Simpson, G. J. Bordonaro, V. I. Merkulov, L. R. Baylor, D. H. Lowndes, *J. Vac. Sci. Technol. B* **2001**, *19*, 573.